

Accepted Manuscript

Title: Ferroelectric-like behaviour of melanin: Humidity effect on current-voltage characteristics

Author: S.L. Bravina P.M. Lutsyk A.B. Verbitsky N.V. Morozovsky

PII: S0025-5408(16)30148-9
DOI: <http://dx.doi.org/doi:10.1016/j.materresbull.2016.03.041>
Reference: MRB 8734

To appear in: *MRB*

Received date: 20-7-2015
Revised date: 14-3-2016
Accepted date: 27-3-2016

Please cite this article as: S.L.Bravina, P.M.Lutsyk, A.B.Verbitsky, N.V.Morozovsky, Ferroelectric-like behaviour of melanin: Humidity effect on current-voltage characteristics, Materials Research Bulletin <http://dx.doi.org/10.1016/j.materresbull.2016.03.041>

This is a PDF file of an unedited manuscript that has been accepted for publication. As a service to our customers we are providing this early version of the manuscript. The manuscript will undergo copyediting, typesetting, and review of the resulting proof before it is published in its final form. Please note that during the production process errors may be discovered which could affect the content, and all legal disclaimers that apply to the journal pertain.

Ferroelectric-like behaviour of melanin: humidity effect on current-voltage characteristics

S. L. Bravina¹, P. M. Lutsyk^{1,2}, A. B. Verbitsky¹, N. V. Morozovsky^{1,*}

¹ *Institute of Physics, NASU, 46 Prospect Nauky, 03680 Kyiv, Ukraine*

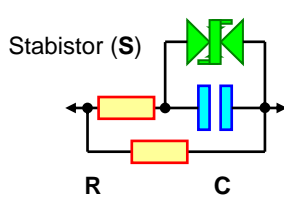
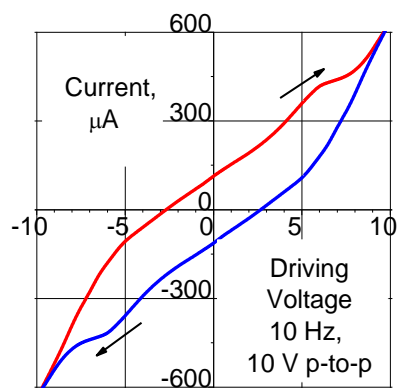
² *School of Engineering and Applied Science, Aston University, Aston Triangle,
B4 7ET Birmingham, UK*

* Corresponding author email: bravmorozo@yahoo.com

Graphical Abstract'



Sample structure

Equivalent non-linear
R-C-S circuitCurrent-voltage loop just after
95 % RH wet air 2 s pulse

HIGHLIGHTS:

Current-voltage dependences (IV-D) of ITO/melanin layer/ITO structures were studied.

Hysteresis voltages of quasistatic IV-D are near to water decomposition potentials.

Short wet air pulse gives rise to displacement current maxima on dynamic IV-D.

Modelling of IV-D by series-parallel RC-circuit with Zener diodes was performed.

As a reason reversible ionic transfer and ferroelectric polarization are considered.

Abstract

The influence of low vacuum on quasistatic current-voltage (I-V) dependences and the impact of wet air pulse on dynamic bipolar I-V-loops and unipolar I-V-curves of fungal melanin thin layers have been studied for the first time.

The threshold hysteresis voltages of I-V dependences are near to the standard electrode potentials of anodic water decomposition.

Short wet air pulse impact leads to sharp increase of the current and appearance of “hump”-like and “knee”-like features of I-V-loops and I-V-curves, respectively.

By treatment of I-V-loop allowing for I-V-curve shape the maxima of displacement current are revealed. The peculiarities of I-V-characteristics were modelled by series-parallel RC-circuit with Zener diodes as nonlinear elements.

As a reason of appearance of temporal polar media with reversible ferroelectric-like polarization and ionic space charge transfer is considered the water-assisted dissociation of some ionic groups of melanin monomers that significantly influences electrophysical parameters of melanin nanostructures.

Keywords: *A. electronic materials, A. organic compounds, D. electrical properties, D. ionic conductivity, D. ferroelectricity.*

1. Introduction

Melanins belong to the class of poly-functional biospherical nanostructural macromolecules [1, 2]. Being hydrated under environment conditions melanin can be considered as natural organic material or synthetic disordered polymer with hybridized mixed electronic-ionic conductivity and can be classified as one of bio-electronic materials [3-9].

Natural melanins are formed due to enzymatic metabolism in the course of melanogenesis process [1, 2] resulting in the mixture of 5,6-dihydroxyindole (DHI) and 5,6-dihydroxyindole-2-carboxylic acid (DHICA) as precursors of main monomeric units, including their various oxidized forms, in particular, 5,6-indolequinone (IQ) and 5,6-indolequinone carboxylic acid (IQCA), and also proteins, lipids and some metal ions.

Synthetic melanins and eumelanins [3-10] can be formed from the same DHI and DHICA basic units taken in definite percentage. DHI and DHICA monomer units can exist in various oxidation states and linked randomly with each other forming quasi-planar oligomers and nanostructures.

The interest for melanin extracted from fungi, plants, animal and human pigments, synthetic melanin and melanin-like materials [9] is connected with their promising applications in photo- and other types of protection [11, 12], neuro-functionality [1, 13], free radical scavenging (in particular, biosensing) [1], and solution of melanoma problem [2]. Melanins including fungal one are widely discussed in terms of prospects for photovoltaic applications [14-17], including development of donor-acceptor compositions of melanin with other compounds [18]. During the decades of research history

of melanin (from 1960s [19, 20]) a multitude of intense studies in the areas of biology [1, 2, 12, 13, 19], chemistry [19, 21, 22] and physics [5-9, 15-18, 20-30] was performed.

Almost 40 years ago melanin was considered as natural amorphous organic semiconductor [28, 29] and lately was proposed as electronic-ionic hybrid conductor for molecular bio-electronics [8, 9]. Later heteropolymer model [1] and nano-scaled aggregate model [24, 25] of eumelanin were proposed and decisive role of chemical disorder was established [22]. Recently, in the issue of current-voltage *dc* and infra-low frequency *ac* characterization, eumelanin was considered as promising for space charge storage based memory devices [26], protonic devices and other bio-electronic applications [27].

Being always partially hydrated, depending on surrounding humidity level melanins possess water molecules influenced physical properties, in particular bistable electrical switching phenomena [28, 29], electrical charge storage effect [3, 4], hopping conductivity and polarization [5-7], hysteretic current-voltage characteristics [26, 27].

Current-voltage characteristics of metal/melanin/metal systems have been investigated in quasistatic mode [26-28]. These results give the information about electrical charge transport and trapping/release processes on their final quasi-stationary stage. In order to obtain more information about the initial stage of charge transfer processes, the study of current-voltage characteristics in dynamic mode is necessary, and so the step from static to dynamic operation mode in melanin conductivity investigations is required.

Earlier we reported [31-37] about the considerable and fast reaction on the humidity impact for a number of nonorganic porous systems, namely zeolite-like Na-Y and mesoporous MCM-41 systems [31], porous Si [33-35] complex metal-oxide ceramics [32, 35] and LiNbO₃-films [36, 37]. These studies proved the efficiency for examining the changes of parameters of bipolar and unipolar dynamic current-voltage characteristics connected with the pulse change of humidity in dynamic operational mode. Therefore, in this paper we present a comparison of the results for static humidity influence on quasistatic current-voltage characteristics and pulse humidity impact on dynamic current-voltage

characteristics of natural melanin. By discussing the obtained results, we aim to provide scientific insights into the mechanisms of electrical transfer supported by equivalent scheme modeling.

2. Experimental

2.1. Sample preparation

The powder of studied fungal melanin was extracted from basidial fungi and purified by Prof. L.F. Gorovyi (Institute of Cell Biology and Genetic Engineering, National Academy of Sciences of Ukraine) [38, 15]. The absorbance, luminescence and photovoltaic properties of the fungal melanin were characterized elsewhere [15]. The melanin powder was dissolved in distilled water at the concentration of 10 mg/ml (1 w/w%), and thin films were obtained by drop casting of water solution on the substrates with In:Sn oxide, ITO, electrodes. The substrates had two strips of ITO electrodes placed in parallel close to each other forming channel that length and width were 100 μm and 4 mm, respectively. The film layer of melanin and ITO electrodes formed planar structure of ITO/melanin/ITO (PSM). The films of melanin were very inhomogeneous by thickness forming dendrite fibers. Average film thickness measured by rod micrometer was about 10 μm .

2.2. Measurements

The basic method applied for examining the influence of static and pulse humidity changes on electrical parameters of PSM was current-voltage characterization. Static humidity influence was studied by its effect on quasistatic current-voltage characteristics. Pulse humidity influence was studied by its impact on dynamic current-voltage characteristics as in our previous studies of porous and mesoporous systems [31-37]. Taking into consideration different levels of photosensitivity depending on various kinds of melanin, different surrounding conditions, material state and type of used sample structure (see e.g. [9, 21, 26]) all the measurements were performed for the samples screened by opaque casing.

Quasistatic current-voltage characteristics (I-V-dependences) were obtained in air atmosphere of relative humidity about 70 % under the normal pressure and under low vacuum 50 Pa (0.38 Torr). The measurements were performed in uni-cycle mode of applied *dc* voltage in the range of (0 - ± 100) V with 3 approximately equal logarithmical steps per decade. Current values were registered with a Keithley 6514 electrometer as current achieves of its quasistatic value after 2-5 min of relaxation.

Bipolar dynamic current-voltage characteristics (I-V-loops) were registered in the multi-cycle mode when applied triangular *ac* driving voltage varied linearly in the range of (0 - ± 10) V with 1 Hz – 1 kHz of frequency.

Unipolar dynamic current-voltage characteristics (I-V-curves) were registered in the sweeping mode when unipolar saw-tooth driving voltage varied in the range (0 - ± 10) V with durability of 50 ms and 10 Hz of repetitive frequency.

For examining effect of step-like change of humidity on the parameters of I-V-loops and I-V-curves the wet air flux pulses with duration of (1-5) s and relative humidity, H_r , near of 95 % were directed on the samples. Direct osciloscopic observations of hydration impact induced variations of I-V-loops and I-V-curves were performed as for metal - ferroelectric - metal [38, 39] and metal - silicon oxide - metal [41, 42] structures. At that the voltage on reference resistor was displayed and measured using two-channel YB54060 (Sinometer Instruments) digital storage oscilloscope.

3. Results

3.1. Quasistatic current-voltage-dependences

Figure 1 presents the quasistatic I-V-dependences obtained for PSM at RT, $H_r = 70\%$ in air under both atmosphere pressure and (Fig. 1, left) and low vacuum (50 Pa) (Fig. 1, right). Positive and negative branches of the both I-V-dependences are similarly shaped and almost symmetric with considerably different forward and backward voltage runs. For the both obtained I-V-dependences low-voltage

hysteretic central region of clockwise path tracing is observed. For both positive and negative branches the hysteresis width at the atmosphere pressure is two times as large as at low vacuum (within the limits of ± 2 V and ± 1 V, respectively) (compare Fig. 1, left and right).

The difference between out-of-hysteresis high-voltage forward and backward runs of I-V-dependence at the atmosphere pressure is considerably higher than at low vacuum due to a change of character of current increase in the range of (1 ÷ 10) V from sharp super-linear (see Fig. 1, left) to nearly linear (see Fig. 1, right). As a result the transition from super-linear to sub-linear behaviour appears in the forward runs of I-V characteristics at the atmosphere pressure. These features in quasistatic I-V characteristics for eumelanin did not observe in air [26] (see the Fig. 3a therein). However the transition took place in [27] as less pronounced but perceptible similar behaviour on the forward runs of I-V characteristics at 90 % H_r (see the Fig. 2b in [27]). On the whole, the quasistatic characteristics obtained at low vacuum are similar to the I-V curves obtained for eumelanin [25]. At that, the differences of 5 orders of magnitude for the current and of 4 orders in hysteresis amplitude value under transition from the atmosphere pressure to low vacuum is in correspondence with the results [5, 21] relatively dehydration influence on conductivity of melanin.

3.2. Dynamic current-voltage characteristics: bipolar loops and unipolar curves

Figure 2 presents the dynamic bipolar I-V-loops (Fig. 2, left) and dynamic unipolar I-V-curves (Fig. 2, right) obtained for the PSM at RT and $H_r^{\min} = 70\%$ before (Fig. 2, bottom) and just after wet air pulse of relatively high ($H_r^{\max} = 95\%$) humidity (Fig. 2, top). The differences of 2-3 orders of magnitude for the currents just after and before wet air pulse impact are in correspondence with similar change of *dc* conductivity of synthetic melanin due to its hydration [5, 21].

The shape of H_r^{\min} bipolar and unipolar I-V characteristics (Fig. 2, bottom) corresponds to series RC-circuit with slightly variable resistive (R) and capacitive (C) components.

Under the action of wet air pulse the increase of I-V-loop average slope and width are observed (Fig. 2, left). These changes are followed by the appearance of characteristic “humps” on forward run and “bends” on backward run of the loop at voltages $V_h \approx \pm 5.8$ V and $V_b \approx \pm 6$ V, respectively (see Fig. 2, left).

At that, the increase of I-V-curve average slope and change of its shape from linear to non-linear with appearance of two “knees” between linear, quasi-saturated and quasi-linear regions is observed (see Fig. 2, right). The “response” time of current rise as the reaction on a wet air pulse is $\tau_1 \approx 1-3$ s.

As the result of temporal hydration, the transformation of I-V-loops corresponds to a decrease of R value and an increase of C value under occurrence of apparent R(V)- and C(V)- non-linearities and the transformation of I-V-curves corresponds to a decrease of R and its jump-like changing in the “knee” region. At that, “retention” time of keeping the hydrated state with high C and low R values is $\tau_2 \approx 10-20$ s depending on wet air pulse duration.

After wet air pulse termination and renewal of initial low H_r^{\min} the shape of I-V-loops and their parameters returned to initial ones with time. For I-V-curves this restoration is also accompanied by decrease of R-non-linearity to the initial value. The “recovery” time of restoring transition to the initial state is $\tau_3 \sim 2-3$ minutes.

Under the frequency decrease sharp endings of I-V-loop elongate considerably due to the decrease of “hump” voltage, V_h , and “bend” voltage, V_b , namely from $V_h \approx V_b \approx 6$ V at 10 Hz (Fig. 2, left) to $V_h \approx V_b \approx 4$ V at 1 Hz. For I-V-curves similar decrease of upper “knee” voltage, V_k , from $V_k \approx 5.5$ V to $V_k \approx 3.5$ V under the same frequency decrease is observed.

Under increase of the driving voltage up to 100 V the almost linear continuation of I-V-loop branches is observed and general shape of dynamic I-V-loop tends to the shape similar to quasistatic I-V-dependences (Fig. 1, right).

4. Discussion

4.1. Quasistatic current-voltage characteristics

Consideration of Figure 1 shows the significant decrease of current and the hysteresis amplitude, on 4-5 orders of magnitude, under the pressure reduce. At that, the hysteresis shape in central part changes insignificantly. The current changes are in agreement with known influence of melanin dehydration/hydration on the conductivity value [5, 21] caused by possible changes in proton migration process [4, 9, 21, 26, 27].

One's attention has been attracted by a decrease of average threshold voltage of hysteresis, V_t , that can be defined as $V_t = (V_t^+ - V_t^-)/2$, where V_t^+ and V_t^- correspond to zero current values of positive and negative branches of I-V-characteristics. At low vacuum, $V_t \approx 0.8$ V that is close to well-known standard electrode potentials of anodic water decomposition: $E^{\circ} = +0.815$ V (corresponding reaction is $2\text{H}_2\text{O} - 4e^- = \text{O}_2\uparrow + 4\text{H}^+$) [43, 44]. Since anodic monatomic oxygen is a strong oxidizer, its evolving results in the electrode polarization, and, for continuation of water anodic oxidation, higher voltage up to +1.5 V is necessary to apply [44]. As the result of hydration, at atmosphere pressure the electrode polarization is higher than under low vacuum, and V_t value increases namely to $V_t \approx 1.5$ V.

For high-voltage parts of I-V-dependence (out-of-hysteresis path), the difference of current value for the forward and backward runs is characteristic. The higher difference under atmosphere pressure than under low vacuum (compare Fig. 1, left and right) is the sign of possible transition from protonic to electronic conductivity preponderance as a consequence of dehydration. The change of I-V-dependence from linear ($I \sim V$) at low vacuum to the power law ($I \sim V^n$, $n = 1.5 \div 2$) at the atmosphere pressure can be connected with injection of charge carriers [45], in particular with proton injection [45]. Under voltage increase, the transition from Ohm's law to Child's law ($I \sim V^2$) [45] is also characteristic to synthetic melanin [28].

4.2. Circuit modeling for dynamic current-voltage characteristics (loops and curves)

Modeling of dynamic I-V-loops was performed aiming to display the changes of effective resistance (R) and capacitance (C) of PSM sample affected by increased humidity. At that, the sample was replaced by combination of parallel RC-circuit (assuming continuous surface and/or bulk conduction) and series RC-circuit (assuming space charge transfer and accumulation either at material/electrode interface or in the vicinity of bulk non-homogeneities resulting in polarization processes).

Zero-voltage ($V_d = 0$) amplitude, width and slope of obtained I-V-loops (Fig. 2) were modelled by parallel RC-circuit (Fig. 3, left). General shape (width, slope change and magnitude) of I-V-loops (Fig. 2) was modelled by series RC-circuits (Fig. 3, middle).

Relative changes of resistance, $\delta R = R(H_r^{\min})/R(H_r^{\max})$, and capacitance, $\delta C = C(H_r^{\max})/C(H_r^{\min})$, connected with H_r increase from its minimal H_r^{\min} to maximal H_r^{\max} values were estimated from corresponding equivalent circuits.

Obtained R and C and also δC and δR values are summarized in Table 1.

The δR and δC values and “recovery” times are about 10 times higher than the ones obtained for nonorganic materials under near the same conditions [31-34].

For the same PSM sample operating at 1 kHz with transformer RC-bridge supplied with oscilloscopic indication under sharp increase and subsequent decrease of H_r value in the limits of (70 - 95) % the values of $\delta C \approx 15$ and $\delta R \approx 35$ were registered.

Observed I-V-nonlinearities cannot be reproduced by linear RC-circuits. Better modeling of general leaf-like shape of bipolar I-V-loop (Fig. 2, left) (but with no “humps”) and peculiarities of unipolar I-V-curve (Fig. 2, right) was performed using combined series-parallel nonlinear circuit (Fig. 3, right). Corresponding I-V-nonlinearity was obtained by two in anti-series connected Zener diodes forming so called stabistor (S) as nonlinear R-element (Fig. 3, right). In particular, taking advantage of Zener diode one can shift the voltage positions of “knees” in I-V-curve and to change the elongation of endings of I-V-loop by corresponding choice of not only R and C values but also stabilization threshold

voltage of the diode. In addition, general shape of quasistatic I-V-dependences with the same current ratio of hysteresis and out-of-hysteresis regions was modeled RC-circuit (Fig. 3, right) at 1Hz of drive voltage frequency.

4.3. Displacement current loop

Elucidation of real shape for displacement current, $I_d(V)$, that contribute to the total current of bipolar I-V-loop can be performed by taking into account and subtraction the conductivity current contribution given by unipolar I-V-curve. I_d -V-loop obtained by such procedure is presented in the Figure 4.

During forward $I_d(V)$ run, one poling maximum (*I*) with voltage position $V_{m1} = \pm 5.5$ V, and during backward $I_d(V)$ run two depoling maxima (*II* and *III*) with voltage positions $V_{m2} \approx \pm 6.5$ V and $V_{m3} \approx \pm 1.5$ V are pronounced. (For maximum *II* slight splitting is distinguished).

V_{m1} is close to the position of the “knee” on unipolar I-V-curve at $V_k \approx \pm 5.5$ V (see Fig. 2, right) that together with position of V_{m3} allows considering the hydration as a common reason of these peculiarities.

The “hump”-like peculiarities of I-V-loop are connected with displacement current maxima $I_D = (dP/dt)$, because hysteretic voltage dependence $P(V)$ under its reversal by external voltage $V(t)$ corresponds to two opposite maxima of $(dP/dV)(dV/dt)$ [39, 40]. Observed for the hydrated PSM samples maxima under forward run of bipolar I_d -V-loop seems to be similar to the maxima of the currents of polarization reversal featuring ferroelectric materials [39, 40].

Besides, it is necessary to note that the maxima on bipolar I-V-loops are characteristic for metal/insulator/semiconductor structures in the case of presence of mobile ionic charge carriers that transfer under internal voltage temporarily increasing the conductivity due to additional displacement current [41, 42].

The maxima *II* and *III* of bipolar I_d -V-loop of PSM observed under the backward run can be related to restoring of initial state of polarization during poling voltage decrease after reaching its maximum. These current maxima are similar to those observed in ferroelectrics with so-called “elastic” domains [40], in particular, in H-bonded molecular crystal triglycine sulphate [47, 48]. These “elastic” domains, which nucleate and start to grow during poling, spontaneously return to its initial state during poling voltage vanishing [47, 48] due to elastic character of domain walls interaction with defects [40].

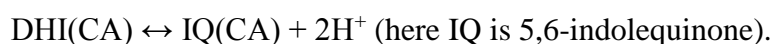
Revealed shape of bipolar I_d -V-loop of hydrated melanin with several current maxima (Fig. 4) is apparently connected with existence of several groups (three in our case) of adsorbed HOH-molecules taking part in polarization process. Depending on degree of bounding with melanin DHI and/or DHICA monomers (more strong or more weak) these molecular groups (three in our case) due to different pinning degree after reorientation behaves themselves similarly to “stable” or “elastic” domains in ferroelectrics [39, 40].

This interpretation is in agreement with the conclusions in Refs. [3] and [4] about relation of “intrinsic” polarisation of natural and synthetic melanins with different states of H₂O-dipoles.

4.4. The ways for water assistant proton conduction and polarization

The water assisted proton (H⁺) conduction can be realized in melanin with participation of basic DHI and/or DHICA monomer molecular units [1, 8, 9, 21, 24, 25, 27] by at least three possible ways.

The **first** one results in proton (H⁺) release by water assisted dissociation connected with ionization of hydroxyl groups, OH⁻, linked with benzene ring of DHI (and/or DHICA):



The **second** one following to [49] results in hydronium ions, H₃O⁺, release by water assisted H⁺ reattachment due to dissociation of carboxylic acid CA by ionization of carboxyl group, COO⁻-H⁺, in DHICA:



The **third** one analogously with [49] results in hydronium ions release by water assisted comproportionation reactions [9] facilitated by IQ as a resultant of first way:



Polar reaction of hydrated melanin seems to be associated with at least two kinds of transformations connected with three above mentioned ways.

The **first kind** of transformation corresponds to second way and so is connected with the break of O-H bonds in hydroxyl groups, OH^- , and temporal dangling of C-O bond in carbonyl group, COO^- , of DHICA.

Dipole moment of DHICA molecule ($5.6 \text{ D} \approx 1.68 \cdot 10^{-29} \text{ C}\cdot\text{m}$, Ref. [50]) is appreciably higher than the dipole moment of polar polyvinylidene fluoride polymer (PVDF, $[\text{CH}_2\text{CF}_2]_n$) ($2.1 \text{ D} \approx 6.3 \cdot 10^{-30} \text{ C}\cdot\text{m}$ on monomer unit). So, polar reaction of melanin can arise from swinging of DHICA molecule during H_3O^+ ion release.

The **second kind** of transformation corresponds to first and third ways and is connected with the doubling of C-O bond owing to reorientation of former O-H bond together with break and flip-over of C-C bonds in benzene ring. At that due to change of bonding in the one of links of benzene ring temporal changing of its charge state takes place that is the reason of temporal decompensation of molecular dipoles and so of temporal dipole moment appearance.

Summing up, polar ferroelectric-like type reaction of hydrated melanin seems to originate from polarization phenomena as a consequence of local disturbance of ionisable radicals ($-\text{H}$ in DHI and $-\text{COOH}$ groups in DHICA) by adsorbed dipolar H_2O molecules (dipole moment $1.84 \text{ D} \approx 5.5 \cdot 10^{-30} \text{ C}\cdot\text{m}$).

Space charge type of hydrated melanin reaction seems to be related to proton transport, and polarization processes appeared either in near electrode region or in the volume in vicinity of inherent to melanin nano-scaled non-homogeneities [1, 23, 25, 29].

Considered perturbations followed by swinging of DHI/DHICA monomers lead to deformation of random inter-monomer bonding in oligomers or in corresponding positions of macromolecules [1] or nanoagregates [22] of melanin. Granting this the perturbations of π -stacking [22, 23] in inter-oligomer assembling of nanoagregates leading to local variation of inter-oligomer distances can also be achieved. So further AFM examination (in the spirit of [22, 23, 25] and similar to electrochemical strain microscopy [51, 52]) directed on detection of hydration-polar and hydration-mechanical reaction of melanin is desirable.

5. Conclusion

Observed changing of quasi-static I-V-dependence peculiarities under transition from the atmosphere pressure to low vacuum is connected with dehydration of melanin. At that two times decrease of the hysteresis width corresponds to drop in twice of electrode polarization potential necessary for anodic water decomposition at low humidity level.

The impact of wet air pulse of (1-5) s duration causes sharp increase of current value and leads to appearance of “hump”-like peculiarities of dynamic bipolar I-V-loops and “knee”-like peculiarities of unipolar I-V-curves. By I-V-loop treatment with accounting I-V-curve shape the maxima of displacement current appeared under hydration are manifested. These maxima are similar to current maxima observed under polarization reversal in ferroelectric materials and under ionic space charge transfer in metal-insulator-semiconductor structures.

Modelling of general shape of I-V-loops and the main peculiarities of I-V-curves of PSM is possible by using linear series-parallel RC-circuit with stabistor as nonlinear element.

For hydrated melanin layer the observed features of quasi-static and dynamic I-V-characteristics are mainly connected with “products” of interaction of melanin monomer units with absorbed water molecules resulted in forming of temporal polar media with enhanced ionic transport, increased dielectric permittivity and reversible polar reaction of ferroelectric-like type.

Absorption of water molecules by melanin macromolecules presumably leads to the water assisted dissociation of melanin monomer units resulting in ionisation of carboxyl and hydroxyl groups of these units that significantly influences electrophysical parameters, in particular charge transfer and polarization ability of PSM.

Obtained results on transformations of I-V-characteristics of PSM under wet air pulse impact demonstrate the efficiency of dynamic electrophysical characterization for studying the effect of fast humidity changes on the properties of melanin. The authors believe that their findings contribute to better understanding of environment surroundings influence on melanin functional abilities and promote further advance of melanin into the class of functional materials for molecular bio-electronics, especially for meso- and nano- scaled flexible organic memories.

Acknowledgements: P.M.L. acknowledges support of EU FP ‘Horizon-2020’ Marie Skłodowska-Curie Individual Fellowship (FOC4SIP).

References

- [1] Prota G. Melanins and melanogenesis. San Diego – London: Academic Press; 1992.
- [2] Lin JY, Fisher DE. Melanocyte biology and skin pigmentation. *Nature* 2007;445:843-50.
- [3] Baraldi P, Capelletti R, Crippa PR, Romeo N. Electrical characteristics and electret behaviour of melanin. *J Electrochem Soc* 1979;126:1207-12.
- [4] Bridelli M, Capelletti R, Crippa PR. Electret state and hydrated structure of melanin. *J Electroanal Chem Interfacial Electrochem* 1981;128:555-67.
- [5] Jastrzebska M, Isotalo H, Paloheimo J, Stubb H. Electrical conductivity and synthetic DOPA-melanin polymer for different hydration states and temperatures. *J Biomater Sci Polym Ed* 1995;7:577-86.
- [6] Jastrzebska MM, Jussila S, Isotalo H. Dielectric response and a.c. conductivity of synthetic dopa-melanin polymer. *J Mater Sci* 1998;33:4023-8.
- [7] Jastrzebska M, Kocot A, Vij JK, Zalewska-Rejda J, Witecki T. Dielectric studies on charge hopping in melanin polymer. *J Mol Struct* 2002;606:205-10.
- [8] Mostert AB, Powell BJ, Gentle IR, Meredith P. On the origin of the electrical conductivity in the bio-electronic material melanin. *Appl Phys Lett* 2012;100: 093701-1-3.
- [9] Mostert AB, Powell BJ, Pratt FL, Hanson GR, Sarna T, Gentle IR, Meredith P. Role of semiconductivity and ion transport in the electrical conduction of melanin. *Proc Natl Acad Sci USA* 2012;109:8943-7.
- [10] Blois MS. The melanins: their synthesis and structure. *Photochem. and Photobiol. Reviews* 1978;3:115-35.
- [11] Riley PA. The evolution of melanogenesis. In: Zeise L, Cedekel MR, Fitzpatrick TB, editors. *Melanin: Its role in human photoprotection*, Overland Park, KS: Valdemar; 1995, p. 11-22.
- [12] Butler MJ, Day AW. Fungal melanins: a review. *Can J Microbiol* 1998;44:1115–36.

- [13] Zucca FA, Giaveri G, Gallorini M, Albertini A, Toscani M, Pezzoli G, et al. The neuromelanin of human substantia nigra: physiological and pathogenic aspects. *Pigm Cell Res* 2004;17:610-17.
- [14] Meredith P, Powell BJ, Riesz J, Vogel R, Blake D, Kartini I, et al. Broadband photon-harvesting biomolecules for photovoltaics. In: Collings AF, Critchley C, editors. *Artificial photosynthesis: from basic biology to industrial application*. Chapt. 3. Weinheim: WILEY-VCH Verlag GmbH & Co. Kga A; 2005, p. 37-65.
- [15] Vertsimakha Ya, Lutsyk P, Kutsenko A. Photovoltaic properties of fungal melanin. *Mol Cryst Liq Cryst* 2014;589:218-25.
- [16] Rosei MA, Mosca L, Galuzzi F. Photoelectronic properties of synthetic melanins. *Synth Met* 1996;76:331-5.
- [17] Davidenko SA, Kurik MV, Piryatinskii YuP, Verbitsky AB. The study of ordered melanin films. *Mol Cryst Liq Cryst* 2008;496:82-9.
- [18] Verbitsky AB, Rozhin AG, Lutsyk PM, Piryatinski YuP, Perminov RJ. Complexation in composite solutions of melanin with 2,4,7-trinitrofluorenone. *Mol Cryst Liq Cryst* 2014;589:209-17.
- [19] Sever RJ, Cope FW, Polis BD. Generation by visible light of labile free radicals in the melanin granules of the eye. *Science* 1962;137:128-9.
- [20] Blois MS, Zahlan AB, Maling JE. Electron spin resonance studies on melanin. *Biophys J* 1964;4:471-90.
- [21] Giacomantonio C. *Charge Transport in Melanin, a Disordered Bio-Organic Conductor*. Honours thesis, University of Queensland, Brisbane, Australia, 2005.
- [22] Meredith P, Sarna T. The physical and chemical properties of eumelanin. *Pigm Cell Res* 2006;19:572-94.
- [23] Tran ML, Powell BJ, Meredith P. Chemical and structural disorder in eumelanins: a possible explanation for broadband absorbance. *Biophys J* 2006;90:743-52.

- [24] Zajac GW, Gallas JM, Cheng J, Eisner M, Moss SC, Alvarado-Swaisgood AE. The fundamental unit of synthetic melanin: a verification by tunneling microscopy of X-ray scattering results. *Biochim Biophys Acta* 1994;1199:271-8.
- [25] Clancy CMR, Simon JD. Ultrastructural organization of eumelanin from *Sepia officinalis* measured by atomic force microscopy. *Biochemistry* 2001;40:13353-60.
- [26] Ambrico M, Cardone A, Ligonzo T, Augelli V, Ambrico P-F, Cicco S, et al. Hysteresis-type current-voltage characteristics in Au/eumelanin/ITO/glass structure: towards melanin based memory devices. *Organic Electron* 2010;11:1809-14.
- [27] Wünsche J, Deng Y, Kumar P, Di Mauro E, Josberger E, Sayago J, et al. Protonic and electronic transport in hydrated thin films of the pigment eumelanin. *Chem Mater* 2015;27: 436-42.
- [28] Osak W, Tkacz K, Czternastek H, Slawinski J. I-V characteristics and electrical conductivity of synthetic melanin. *Biopolymers* 1989;28:1885-90.
- [29] McGinness J, Corry P, Proctor P. Amorphous semiconductor switching in melanins. *Science* 1974;183:853-5.
- [30] Filatovs J, McGinness JE, Proctor PH. Thermal and electronic contributions to switching in melanins. *Biopolymers* 1976;15:2309-12.
- [31] Bravina SL, Morozovsky NV, Tel'biz GM, Shvets AV. Electrophysical characterization of meso-porous structures. *Materials of Internat. conf. on optical diagnostics, materials and devices for opto-, micro and quantum electronics. Ukraine, Kiev: SPIE; 1999, p. 95.*
- [32] Bravina SL, Morozovsky NV, Khaikina EG. Temperature and humidity sensors with response to frequency conversion based on porous ceramics. *Materials of 12th IEEE international symposium on the application of ferroelectrics (ISAF). Hawaii; 2000.*
- [33] Bravina SL, Morozovsky NV. Humidity effect on the current-voltage characteristics and transient currents of porous materials and smart high-speed humidity sensors. *Materials of 2-nd open French-Ukrainian meeting on ferroelectricity and ferroelectric thin films. Dinard, France; 2002.*

- [34] Bravina S L, Morozovsky NV, Boukherroub R. Dynamic electrophysical characterization of porous silicon based humidity sensing. *Semiconductor Phys Quantum Electron and Optoelectron* 2006;9:74-83.
- [35] Bravina S, Morozovsky N, Pasechnik L, Khaikina E, Boukherroub R, Dogheche E, Remiens D. Dynamic characterization of nano- and mesoporous media under fast humidity impact. *Materials of 1-st Internat. conf. on multifunctional and nano-materials. Tours, France; 2009.*
- [36] Bravina SL, Morozovsky NV, Dogheche E, Remiens D. Fast humidity sensing and switching of LiNbO₃ films on silicon. *Materials of Internat. conf. CEROM8; 2010, p. 269-70.*
- [37] Bravina SL, Morozovsky NV, Dogheche E, Remiens D. Fast humidity sensing and switching of LiNbO₃ films on silicon. *Mol Cryst Liq Cryst* 2011;535:196-203.
- [38] Seniuk OF, Gorovyi LF, Palamar LA, Krul NI. Effects of melanin-glucan complex, isolated from polypore fungi, on the lifespan of female icr mice, *Problemy Starenija i Dolgoletia* 2014;23:11-27. (in Russian)
- [39] Burfoot JC. *Ferroelectrics. an introduction to the physical principles.* London: Van Nostrand; 1966.
- [40] Burfoot JC, Taylor GW. *Polar dielectrics and their applications.* London-New Jersey: Macmillan Press LTD; 1979.
- [41] Chou NJ. Application of triangular voltage sweep method to mobile charge studies in MOS-structures. *J Electrochem Soc* 1971;118:601-13.
- [42] Kuhn M, Silversmith DJ. Ionic contamination and transport of mobile ions in MOS-structures. *J Electrochem Soc* 1971;118:966-70.
- [43] Pilipenko AT, Potchinok VYa, Sereda IP, Shevtshenko FD. *Elementary Chemistry Reference book.* Ukraine, Kiev: Scientific Idea; 1985. (in Russian)
- [44] Pavlov NN. *Inorganic chemistry: theoretical foundations of inorganic chemistry. properties of elements and their connections.* Moscow: Higher School; 1986. (in Russian)

- [45] Lampert MA, Mark P. Currents injection in solids. New York and London: Academic Press; 1970.
- [46] Glasser L. Proton conduction and injection in solids. Chem Rev 1975;75:21-65.
- [47] Fatuzzo E, Merz WJ Switching mechanism in triglycine sulfate and other ferroelectrics. Phys Rev 1959;116:61-8.
- [48] Taylor JW. Partial switching behavior in ferroelectric triglycine sulfate. J Appl Phys 1966;37:593-9.
- [49] Pethig R. Dielectric and electronic properties of biological materials. Chichester: John Wiley and Sons; 1979.
- [50] Riesz J. The spectroscopic properties of melanin. PhD thesis. University of Queensland; 2007. www.physics.uq.edu.au/people/powell/Jenny-Riesz-Phd-thesis.pdf
- [51] Morozovska AN, Eliseev EA, Balke N, Kalinin SV. Local probing of ionic diffusion by electrochemical strain microscopy: spatial resolution and signal formation mechanisms. J Appl Phys 2010;108:053712-1-21.
- [52] Balke N, Jesse S, Morozovska AN, Eliseev EA, Chung DW, Kim Y, et al. Nanometer-scale electrochemical intercalation and diffusion mapping of Li-ion battery materials. Nature nanotechnology, 2010;5:749-54.

Figure captions page:

Fig. 1. Quasistatic unipolar current-voltage dependences of ITO/Melanine/ITO planar structure at atmosphere air pressure (left) and at low vacuum (right). Positive and negative runs marked by (+) and (-) respectively. Poling run marked by open symbols.

Fig. 2. Dynamic bipolar current-voltage loops (left) and unipolar current-voltage curves (right) of ITO/Melanine/ITO planar structure at 10 Hz of operating frequency (initial below and just after wet air pulse finishing above).

Fig. 3. Modelling equivalent circuits: parallel (left) and series (middle) linear RC and combined nonlinear RCS (right).

Fig. 4. Dynamic bipolar displacement current-voltage loop obtained as difference of bipolar I-V-loop (Fig. 2a) and unipolar I-V-curve (Fig. 2b). One poling maximum (I) under forward run and two depoling maxima (II) and (III) under backward run are well distinguished.

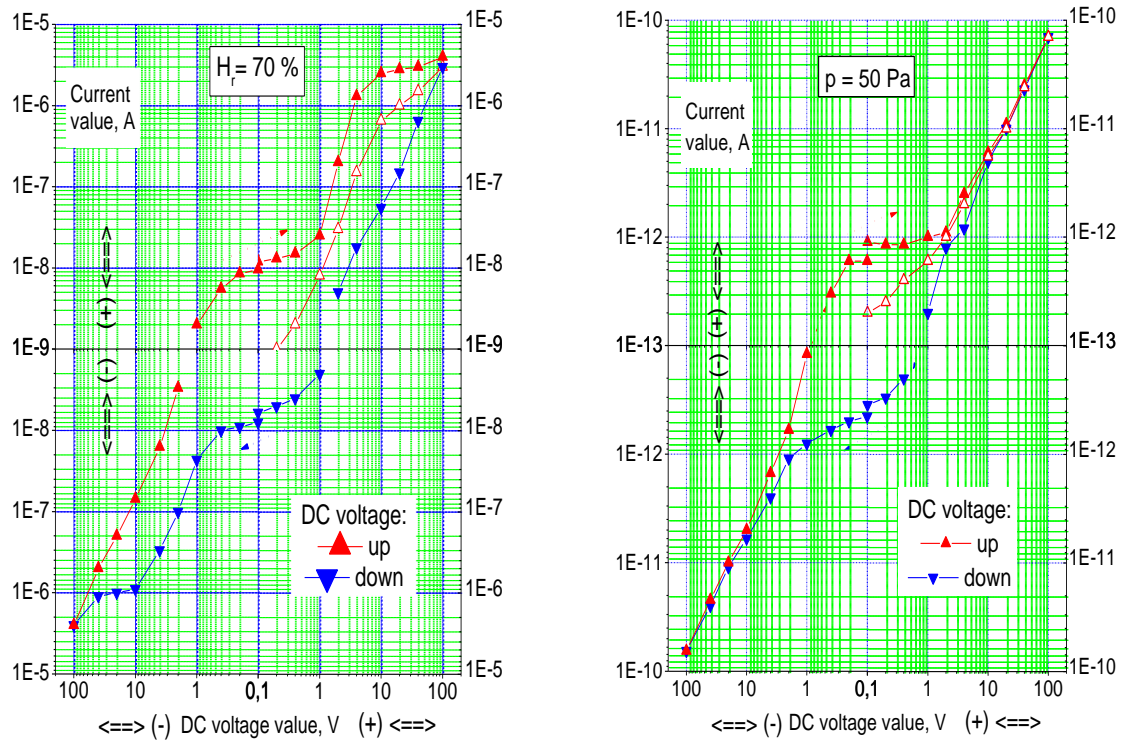


Fig. 1.

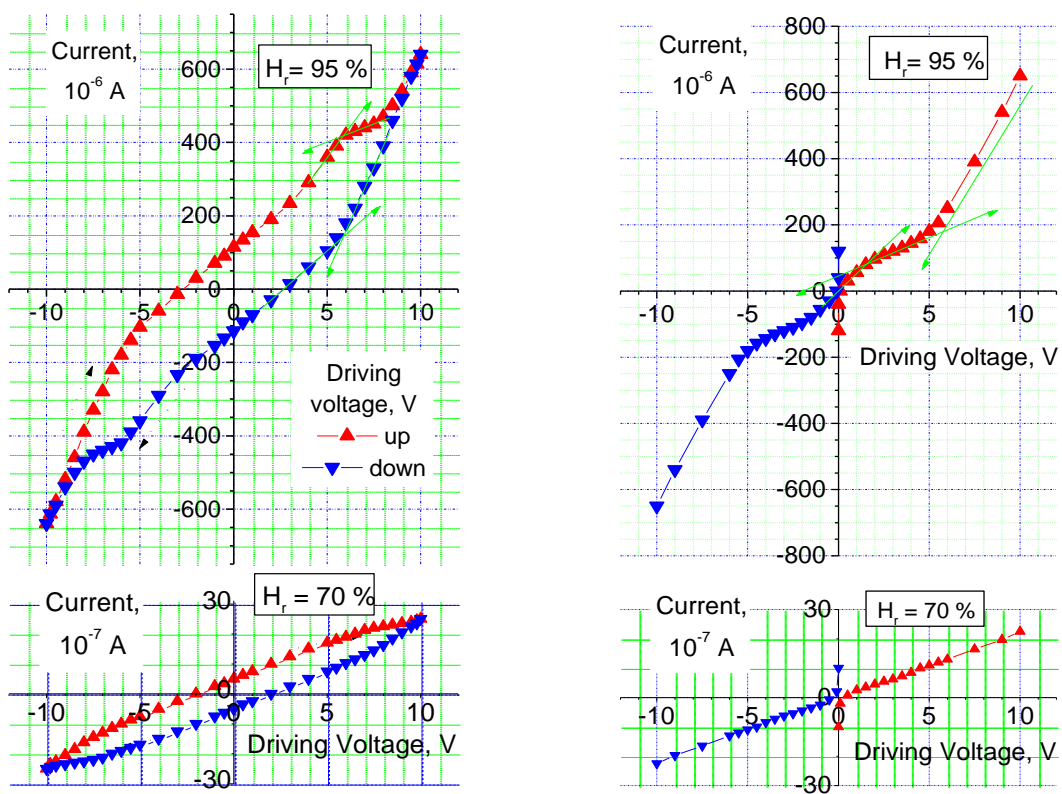


Fig. 2.

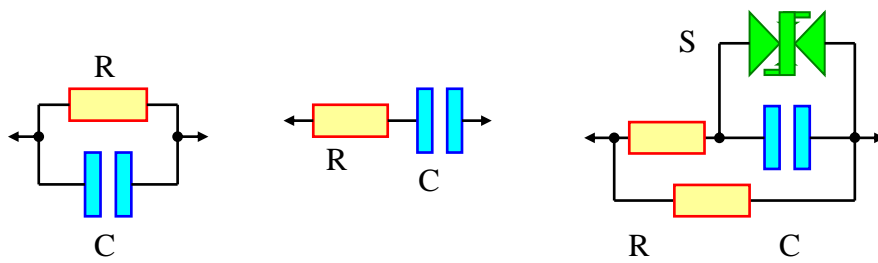


Fig. 3.

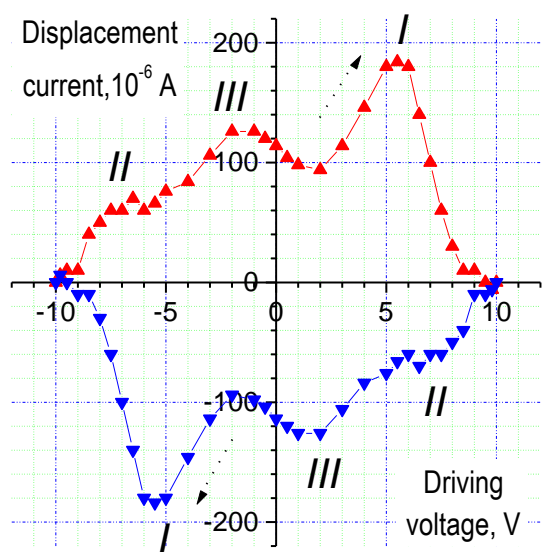


Fig. 4.

Table 1 Types of equivalent RC circuit, effective resistance (R) and capacitance (C) at different humidity levels and relative changes, δR and δC , caused by humidity impact.

RC-circuit		$H_r^{\min} = 70\%$	$H_r^{\max} = 95\%$	Relative change
parallel	R, kOhm	4000	25	160
	C, μF	0.02	4.4	220
series	R, kOhm	3300	15	220
	C, μF	0.025	3.3	132